Plasma gasification performances of various raw and torrefied biomass materials using different gasifying agents

Kuo, Po Chih; Illathukandy, Biju; Wu, Wei; Chang, Jo Shu

DOI
10.1016/j.biortech.2020.123740

Publication date
2020

Document Version
Final published version

Published in
Bioresource Technology

Bioresource Technology 314 (2020) 123740

Contents lists available at ScienceDirect

Bioresource Technology

journal homepage: www.elsevier.com/locate/biortech

Plasma gasification performances of various raw and torrefied biomass materials using different gasifying agents

Po-Chih Kuo[a,*], Biju Illathukandy[b], Wei Wu[c], Jo-Shu Chang[c,d,e]

[a] Process and Energy Department, Faculty of 3mE, Delft University of Technology, Leeghwaterstraat 39, 2628, CB, Delft, The Netherlands
[b] Centre for Rural Development & Technology, Indian Institute of Technology, Delhi, India
[c] Department of Chemical Engineering, National Cheng Kung University, Tainan 70101, Taiwan
[d] Department of Chemical and Materials Engineering, Tunghai University, Taichung 407, Taiwan
[e] Research Center for Smart Sustainable Circular Economy, Tunghai University, Taichung 407, Taiwan

GRAPHICAL ABSTRACT

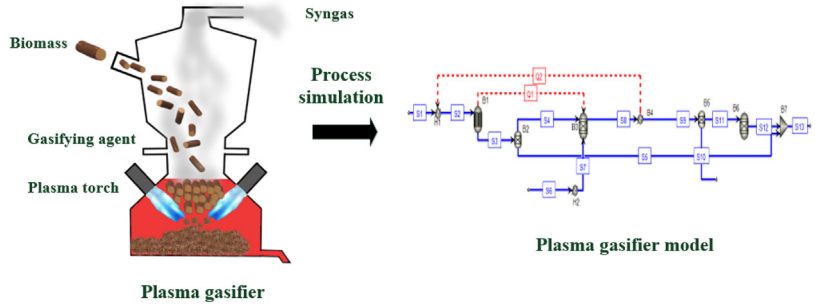

ARTICLE INFO

Keywords:
Plasma gasification
Torrefied biomass
Thermodynamic analysis
NO_x and SO_x precursors
Plasma energy to syngas production ratio (PSR)
Plasma gasification efficiency (PGE)

ABSTRACT

Plasma gasification of raw and torrefied woody, non-woody, and algal biomass using three different gasifying agents (air, steam, and CO_2) is conducted through a thermodynamic analysis. The impacts of feedstock and reaction atmosphere on various performance indices such as syngas yield, pollutant emissions, plasma energy to syngas production ratio (PSR), and plasma gasification efficiency (PGE) are studied. Results show that CO_2 plasma gasification gives the lowest PSR, thereby leading to the highest PGE among the three reaction atmospheres. Torrefied biomass displays increased syngas yield and PGE, but is more likely to have a negative environmental impact of N/S pollutants in comparison with raw one, especially for rice straw. However, the exception is for torrefied grape marc and macroalgae which produce lower amounts of S-species under steam and CO_2 atmospheres. Overall, torrefied pine wood has the best performance for producing high quality syngas containing low impurities among the investigated feedstocks.

1. Introduction

Plasma technology has been recently considered as a promising way to be applied to a wide range of biomass conversion processes such as gasification (Diaz et al., 2015), pyrolysis (Shie et al., 2010; Huang et al., 2013), and liquefaction (Xi et al., 2017). Among them, the interest on plasma gasification has gained increasing attention as an environmentally friendly and efficient approach to convert the carbon-based materials such as municipal solid waste, plastics, tires, and biomass into synthesis gas (i.e. H_2 and CO), which can be further utilized

* Corresponding author.
E-mail address: p.c.kuo@tudelft.nl (P.-C. Kuo).

https://doi.org/10.1016/j.biortech.2020.123740
Received 14 May 2020; Received in revised form 20 June 2020; Accepted 22 June 2020
Available online 27 June 2020

for the synthesis of liquid fuels via the Fischer Tropsch (FT) technology (Kim et al., 2013) or power generation through combustion or fuel cell technologies (Liu and Aravind, 2014).

In recent years, plasma gasification of biomass has been considered as an alternative to the traditional biomass gasification technologies because it is featured by higher operating temperature (up to ~5000 °C) and heating rate, thereby improving the gasification reaction rates and gas productivity (Favas et al., 2017; Shie et al., 2010). Another important merit accompanied by plasma gasification of biomass is that the extent of tar cracking reaction can be intensified to completely destroy tars under high temperature plasma, thereby leading to low concentration of tars, especially heavy components, in the product gas (Shie et al., 2010; Favas et al., 2017; Munir et al., 2019). This implies, therefore, that the production of syngas from a plasma gasifier is possible to be directly applied for internal combustion engine and solid oxide fuel cell (SOFC) without additional tar removal processes (Liu and Aravind, 2014; Rios et al., 2018).

In reviewing past literature, it could be seen that there were few experimental studies performed by various researchers to evaluate the performance of biomass plasma gasification. For example, Hlina et al. (2006) conducted a plasma gasification of wood by using a plasma torch with DC electric arc to produce plasma. The tar content in syngas from the plasma gasifier was found to be lower than 10 mg Nm^{-3}. Hlina et al. (2014) also studied plasma gasification of wood sawdust (spruce) and wood pellets under a reaction temperature between 1200 and 1400 °C. It was reported that high-quality syngas (~51 vol% CO and 42% H_2) with negligible content of tars were produced from the wood sawdust and wood pellets, and the wood sawdust had the highest plasma gasification efficiency (PGE) (~50%). Diaz et al. (2015) compared the performance of six different types of biomass materials in two-stage plasma gasification with steam. It was indicated that the concentration of H_2 in the syngas exceeding 52 vol% with low content of hydrocarbons (lower than 0.4%) was obtained and the PGE was between 24 and 51%. Apart from the experimental works, attempts in thermodynamic modeling of biomass plasma gasification have also been investigated. To illustrate, Janajreh et al. (2013) simulated the plasma gasifier with a DC arc plasma torch under an air–steam environment in Aspen Plus and evaluated its performance for various biomass samples. Based on this simulation, the obtained values of PGE from highest to lowest were: pine needles (47.00%) > treated wood (46.20%) > untreated wood (43.50%) > plywood (40.51%) > algae (38.27%). Favas et al. (2017) performed the plasma gasification of three kinds of biomass materials with air and steam, using Aspen Plus. The results revealed that the higher the equivalence ratio (ER), the lower the lower heating value (LHV) of the product gas, and the same trend was also found when the steam plasma gasification was conducted. More recently, Ismail et al. (2019) numerically developed a Eulerian model for simulating the plasma gasification of forest residues with air and steam. It was shown that higher ERs had a negative impact on the formation of syngas and its LHV, but a positive one on the carbon conversion efficiency due to a greater extent of the oxidation reaction.

These earlier works show that converting biomass into syngas by thermal plasma is favorable for high quality syngas production with a fairly low-level concentration of tars. Nevertheless, some unfavorable characteristics inherently exist in raw biomass such as high moisture content, hygroscopic nature, low calorific values, low bulk and energy density, and poor grindability, etc. (Guo et al., 2017; Chen and Kuo, 2011), thereby making raw biomass impractical for utilization, storage, and transportation. As a result, torrefied biomass, which is produced by a torrefaction pretreatment, has recently become an attractive alternative to the raw one. Torrefaction is a mild pyrolysis process carried out at a temperature between 200 and 300 °C under an inert or minimized oxidative atmosphere (Kuo et al., 2014). Many researchers have investigated the applications of torrefied biomass for gasification technology (Kuo et al., 2014; Marcello et al., 2017; Pinto et al., 2017a,b; Weiland et al., 2014; Xue et al., 2014) and their results verified that torrefied biomass has benefits for gasification performance. However, to this end, an examination of the past literature reveals that no works have been done to evaluate the utilization of torrefied biomass in a plasma gasifier, nor those that compare the performance of plasma gasification between raw and torrefied biomass. For the foregoing reasons, the purpose of this study is to first develop the plasma gasifier in an Aspen Plus simulator and then analyze the plasma gasification characteristics of various types of raw and torrefied biomass under three reaction atmospheres, namely air, steam, and CO_2.

On the other hand, nitrogenous and sulfur-containing species such as NH_3, HCN, H_2S, and COS are poisons for catalysts in the chemical synthesis reactors or mainly precursors to lead to the formation of NO_X and SO_X during the syngas combustion (Ren et al., 2017). An initial understanding of the release of nitrogenous and sulfur-containing pollutants during gasification is helpful for choosing a suitable fuel to further syngas combustion applications. Therefore, the formation of NH_3, HCN, H_2S, and COS from raw and torrefied biomass during the plasma gasification is also explored and compared in detail. The impact of ER, steam to carbon ratio (S/C), and CO_2 to carbon ratio (CO_2/C) on the various performance indices of the plasma gasification such as LHV of the product gas, plasma energy to syngas production ratio (PSR), and PGE are investigated to find the optimal operating conditions and feedstocks.

2. Materials and methods

2.1. System description

The simulation model is carried out using Aspen Plus V8.8. The following assumptions are considered: (1) the process is in state-steady; (2) the solid and gaseous phases are in a state of thermodynamic equilibrium (Kuo et al., 2014); (3) the product gas comprises H_2, CO, CO_2, H_2O, CH_4, N_2, NH_3, HCN, H_2S, and COS (Mazzoni and Janajreh, 2017; Kuo et al., 2014); (4) the heat losses of the plasma gasifier are neglected (Mazzoni and Janajreh, 2017); and (5) char is assumed as graphitic carbon (Janajreh et al, 2013; Kuo et al., 2014). The Peng-Robinson equation of state with the Boston-Mathias alpha function (PR-BM) model is selected as property methods (Kuo et al., 2014). The feedstock is established as a non-conventional component based on proximate and elemental analyses. The HCOALGEN model is selected to estimate the heat of combustion, heat of formation, and heat capacity of the feedstock, while the DCOALIGT model is used to calculate the density of the feedstock (Kuo et al., 2014). As shown in the process flow diagram for the plasma gasifier, the feedstock (S1) enters the system at ambient conditions (i.e. 25 °C and 1 atm). It is then fed to a RYield block (B1) where the non-conventional fuel is decomposed to conventional components, including C, H_2, N_2, O_2, S, ash, and moisture (S2) by using a calculator, which is implemented by the FORTRAN statement. Both the conventional components and plasma gas (S6) are then sent to a RGibbs reactor (B3) at a high temperature of 2500 °C (Minutillo et al., 2009; Janajreh et al, 2013; Mazzoni and Janajreh, 2017), in which the chemical and multiphase equilibrium calculations are solved by the Gibbs free energy minimization, which is reported elsewhere in a previous study (Kuo et al., 2014). Meanwhile, the plasma gas is heated up to 4000 °C in a heater (H2) in which a DC plasma torch is simulated (Minutillo et al., 2009; Janajreh et al, 2013; Mazzoni and Janajreh, 2017). A separator (B5) is then used to remove the residual slag from the product gas. The product gas subsequently flows to another RGibbs reactor (B6) at a temperature of around 1000 °C to complete the gasification reaction. The key chemical reactions occurring in the plasma gasifier are listed in Table 1 (Park et al., 2008; Gai et al., 2014; Kuo et al., 2014).

Table 1
A list of key chemical reactions occurring during the plasma gasification (Park et al., 2008; Gai et al., 2014; Kuo et al., 2014).

Reaction name	Chemical reaction	Reaction number
Devolatilization	$CH_xO_yN_zS_w \rightarrow char + volatiles$	R1
Oxidation	$C + 0.5\,O_2 \rightarrow CO, \quad \Delta H^0 = -268\ kJ\ mol^{-1}$	R2
	$C + O_2 \rightarrow CO_2, \quad \Delta H^0 = -406\ kJ\ mol^{-1}$	R3
Water gas reaction	$C + H_2O \rightarrow CO + H_2, \quad \Delta H^0 = 131.4\ kJ\ mol^{-1}$	R4
Water gas shift reaction	$CO + H_2O \leftrightarrow CO_2 + H_2, \quad \Delta H^0 = -42\ kJ\ mol^{-1}$	R5
Boudouard reaction	$C + CO_2 \rightarrow 2\,CO, \quad \Delta H^0 = 172.6\ kJ\ mol^{-1}$	R6
Methanation reaction	$C + 2\,H_2 \leftrightarrow CH_4, \quad \Delta H^0 = -75\ kJ\ mol^{-1}$	R7
Steam methane reforming	$CH_4 + H_2O \leftrightarrow CO + 3H_2, \quad \Delta H^0 = 206\ kJ\ mol^{-1}$	R8
Nitrogenous species formation	$N_2 + 3H_2 \rightarrow 2NH_3$	R9
	$Char\text{-}N \xrightarrow{H} HCN$	R10
	$HCN + H_2O \rightarrow NH_3 + CO$	R11
Sulphur species formation	$H_2S + CO_2 \rightarrow COS + H_2O$	R12
	$H_2S + CO \rightarrow COS + H_2$	R13

2.2. Model validation

The simulation model of the plasma gasifier is validated by comparing it with the results obtained from Minutillo et al. (2009) and Janajreh et al. (2013). In the study of Minutillo et al. (2009), the refuse derived fuel was used as the feedstock for plasma gasification with air as the medium, while various feedstocks were gasified under a mixture of air–steam environment in the study of Janajreh et al. (2013). Table 2 shows a comparison of the product gas composition and plasma torch power between the present model and the published literature under the same operating conditions and it is clear that the predicted values from the developed plasma gasifier at different plasma gas to fuel ratios are in good agreement with the data available from the literature. The present model can thus be utilized to predict the performance of the plasma gasification process for various raw and torrefied biomass materials.

2.3. Biomass materials

Five raw (R) and torrefied (T) biomasses, i.e. pine wood chips (PW), rice straw (RS), forest residues (FR), grape marc (GM), and macroalgae (MA) (*Oedogonium intermedium*) are selected as the feedstock in this work. The property data of PW, RS, FR is collected from the studies of Phanphanich and Mani (2011), Kai et al. (2019), and Li et al. (2015) respectively, while that of GM and MA is obtained from the work of Guo et al. (2017). The torrefaction temperature and residence time of 275 °C and 30 min, respectively, are chosen for plasma gasification of torrefied biomass in this work (Misljenovic et al., 2014; Huang et al., 2019). The proximate analysis, elemental analysis, and place of origin of raw and torrefied biomass are presented in Table 3.

2.4. Process parameters and performance indices

Three different operating parameters (i.e. gasifying agents: air, steam, and CO_2), including equivalence ratio (ER), steam-to-carbon (mass flow rate) ratio (S/C), and CO_2-to-carbon (mass flow rate) ratio (CO_2/C) are used for biomass plasma gasification. In this study, operational parameters in the plasma gasifier with respect to the ER, S/C, and CO_2/C are 0.2–0.4 (interval: 0.02), 1–4 (interval: 0.25), and 1–4 (interval: 0.25), respectively. They are defined as follows:

$$ER = \frac{(\dot{m}_{air}/\dot{m}_{biomass})_{actual}}{(\dot{m}_{air}/\dot{m}_{biomass})_{\text{stoichiometric}}} \tag{1}$$

$$S/C = \frac{\dot{m}_{steam}}{y_c \times \dot{m}_{biomass}} \tag{2}$$

$$CO_2/C = \frac{\dot{m}_{CO_2}}{y_c \times \dot{m}_{biomass}} \tag{3}$$

where $\dot{m}_{biomass}$, $\dot{m}_{air}$, $\dot{m}_{steam}$, $\dot{m}_{CO_2}$ are the mass flow rate of biomass, air, steam, and carbon dioxide (kg s^{-1}), respectively, and y_c is the carbon content in the feedstock (wt%).

To evaluate and compare the performance of plasma gasification between raw and torrefied biomass, different performance indices such

Table 2
The comparison of predicted results with the data from literature for model validation.

Feedstock	Gasifying agents	Plasma gas/fuel ratio	Source	Gas composition (vol. %)									Torch power (MW)
				H_2	CO	CO_2	CH_4	H_2O	N_2	H_2S	COS	HCl	
RDF[a]	Air	0.782	Minutillo et al. (2009)	21.04	33.79	0	5.97	11.68	26.97	0.22	0.02	0.32	4.26
			Present model	21.02	33.79	0	5.99	11.69	26.96	0.22	0.02	0.32	4.25
RDF[a]	O_2 (vol 40%)	0.643	Minutillo et al. (2009)	31.49	38.73	0.42	0	12.50	16.32	0.22	0.01	0.31	3.44
	N_2 (vol 60%)		Present model	31.51	38.71	0.44	0	12.47	16.31	0.22	0.01	0.31	3.43
RDF[a]	Air	0.505	Minutillo et al. (2009)	28.65	37.37	1.41	0	14.91	17.12	0.22	0.01	0.31	2.75
	O_2	0.207	Present model	28.85	37.18	1.60	0	14.71	17.12	0.22	0.01	0.31	2.75
Coal	Air	1.31	Janajreh et al. (2013)	50.28	40.89	0.05	0	0.72	7.83	0.20	0.01	0	16.65
	Steam	0.7	Present model	50.35	40.75	0.07	0	0.79	7.82	0.20	0.01	0	16.69
MSW[b]	Air	0.36	Janajreh et al. (2013)	43.50	34.50	0.03	0.01	16.22	5.63	0.09	0	0	4.06
	Steam	0.56	Present model	43.50	34.40	0.05	0.01	16.27	5.69	0.08	0	0	4.07
Wood	Air	1.38	Janajreh et al. (2013)	22.68	36.45	0.65	0	5.31	34.90	0	0	0	7.84
			Present model	22.74	36.43	0.64	0	5.30	34.89	0	0	0	7.85

[a] RDF: refused-derived fuel.
[b] MSW: municipal solid waste.

Table 3
Chemical properties of raw and torrefied biomass (at 275 °C for 30 min) materials used in the simulation.

Feedstocks	RPW	TPW	RRS	TRS	RGM	TGM	RFR	TFR	RMA	TMA
Proximate analysis (wt%, dry basis)										
Moisture	6.69	2.46	4.35	1.75	2.87	2.59	6.30	4.20	7.55	3.38
Volatile matter	85.98	76.40	78.26	72.60	66.56	52.83	74.71	64.30	72.50	50.59
Fixed carbon	13.75	23.25	12.09	16.42	27.67	39.32	22.95	32.88	19.08	35.54
Ash	0.27	0.35	9.65	10.98	5.77	7.85	2.35	2.82	8.42	13.87
Elemental analysis (wt%, dry-ash-free)										
C	47.31	55.20	42.57	49.02	53.65	64.93	52.10	59.50	49.13	63.86
H	6.65	6.23	5.84	5.16	6.80	6.55	6.10	5.60	7.22	6.24
N	0.17	0.20	2.13	5.20	2.32	2.85	0.50	0.60	4.61	6.76
O	45.87	38.37	49.33	40.46	37.10	25.55	41.30	34.30	38.88	23.00
S	–	–	0.13	0.16	0.14	0.12	–	–	0.15	0.14
HHV (MJ kg^{-1})	18.46	21.82	16.60	18.82	21.51	25.47	20.86	23.67	19.59	22.93
LHV (MJ kg^{-1})	16.83	20.39	15.21	17.64	20.02	24.07	19.36	22.33	17.95	21.67
Reference	Phanphanich and Mani, (2011)		Kai et al. (2019)		Guo et al. (2017)		Li et al. (2015)		Guo et al. (2017)	
Place of origin	Oglethorpe, Georgia		Shenyang, China		Adelaide, Australia		–		Queensland, Australia	

Note: RPW: raw pine wood chips; TPW: torrefied pine wood chips; RRS: raw rice straw; TRS: torrefied rice straw; RGM: raw grape marc; TGM: torrefied grape marc; RFR: raw forest residues; TFR: torrefied forest residues; RMA: raw macroalgae; TMA: torrefied macroalgae

as syngas yield (Nm^3 kg-$fuel^{-1}$), lower heating value (LHV) of the product gas, plasma energy to syngas production ratio (PSR), plasma gasification efficiency (PGE) are calculated as follows (Kaewluan and Pipatmanomai, 2011):

$$LHV_{gas} = 10.79Y_{H_2} + 12.62Y_{CO} + 35.81\,Y_{CH_4} \quad (4)$$

$$PSR = \frac{E_{plasma}}{\dot{m}_{syngas}} \quad (5)$$

$$E_{plasma} = \frac{W_{torch}}{\eta_{torch} \times \eta_{electric}} \quad (6)$$

$$PGE\,(\%) = \frac{G_P \times LHV_{product\ gas}}{(\dot{m}_{biomass} \times LHV_{biomass}) + E_{plasma}} \times 100\% \quad (7)$$

where Y_{H_2}, Y_{CO}, Y_{CH_4} are the volume fractions of H_2, CO, CH_4, respectively in the product gas based on a dry basis. E_{plasma} is the plasma energy (MW), G_P is the yield of product gas (Nm^3 kg-$fuel^{-1}$), $LHV_{biomass}$ and LHV_{gas} are the LHV of biomass (MJ kg^{-1}) and product gas (MJ Nm^{-3}), respectively. W_{torch} is the plasma torch power (MW). η_{torch} and $\eta_{electric}$ represent the plasma torch efficiency (90%) (Minutillo et al., 2009) and electrical efficiency (39%) (Oh et al., 2018), respectively.

3. Results and discussion

3.1. Characterization of product gas from the plasma gasification

A comparison of product gas characteristics from the plasma gasification under three different atmospheres, namely, air, steam, and CO_2, between several types of biomass (RPW, TPW, RRS TRS, RGM, TGM, RFR, TFR, RMA, and TMA) is first investigated. The syngas composition from each feedstock is shown in Fig. 1, while the emissions of nitrogenous (NH_3 and HCN) and sulfur (H_2S and COS) impurities are shown in Figs. 2 and 3, respectively.

3.1.1. Syngas composition

Fig. 1 depicts the dry-basis concentrations of H_2 and CO from the plasma gasification as a function of ER, S/C ratio, and CO_2/C ratio. For the air plasma gasification, H_2 concentration decreases with increasing ER for all types of raw and torrefied biomass. This is because a higher ER means more oxygen supplied to the plasma gasifier, causing a greater extent of the combustion reaction. Similar to the trend of H_2 concentration, CO concentration drops along with ER for all types of raw biomass. These trends of H_2 and CO for raw biomass are consistent with the results reported by Favas et al. (2017). Notably, for TGM, TFR, and TMA, the trend of CO concentration is first insensitive to ER (at lower ERs) and then declines in a significant way, thereby resulting in a rise in CO_2 concentration. For instance, as the ER increases from 0.2 to 0.28, 0.2–0.24, and 0.2–0.28, the CO concentration only decreases from 33.19 to 33.10% for TGM, 37.73 to 37.35% for TFR, and 32.51 to 31.31% for TMA, respectively.

It is well known that the chemical and physical properties of raw biomass are changed after torrefaction. The carbon–hydrogen–oxygen (C–H-O) ternary and the van Krevelen diagrams can be used to understand how torrefaction affects the elemental compositions of biomass. When the raw biomass undergoes torrefaction at 275 °C for 30 min, the C–H-O ternary diagram shows that torrefaction results in an increase in the carbon content and a decrease in the hydrogen and oxygen contents in the feedstock, while the van Krevelen diagram clearly demonstrates that torrefied biomasses have lower atomic hydrogen to carbon (H/C) and the atomic oxygen to carbon (O/C) ratios. As a result, it can be seen that air plasma gasification from all types of raw biomass produces higher H_2 concentration as compared to torrefied one due to a higher moisture and hydrogen content (Table 3). In contrast, using torrefied biomass as the feedstock gives a higher CO concentration because of higher carbon content. The exception is for TGM when ER ranges from 0.2 to 0.24.

In examining the syngas composition of steam plasma gasification from raw and torrefied biomass, both the concentrations of H_2 and CO are very dependent on S/C ratio, no matter what fuels are examined. By virtue of involving both water gas reaction (R4) and water–gas shift reaction (R5) in the plasma gasifier, increasing the S/C ratio leads to higher H_2 concentration, whereas it results in lower CO concentration and higher CO_2 concentration. These results are in accordance with the phenomenon in steam plasma gasification of three different biomasses found by Favas et al. (2017). It is worth noting that using torrefied biomass to replace raw biomass as a fuel in the plasma gasification with steam could not improve the H_2 concentration except for TGM, in which its H_2 concentration is somewhat improved by factors of 0.08–0.96% when the S/C ratio is larger than 1.25. As a whole, H_2 concentration ranges from 52.30 to 63.25% within the investigated S/C ratio range. In contrast to the H_2 concentration, CO concentration of all torrefied biomass types is considerably enhanced up to 3.10–14.76% due to the enrichment of carbon through torrefaction.

Once the raw and torrefied biomasses are gasified in the CO_2 atmosphere, the Boudouard reaction (R6) and reverse water–gas shift reaction (R5) will be dominant in the plasma gasifier. The rise in CO_2/C ratio is found to decrease H_2 formation as a result of (R5), while CO concentration first increases substantially until it reaches a maximum value, and then it decreases with further increases in the CO_2/C ratio. This arises from the fact that R6 is mainly driven in the plasma gasifier

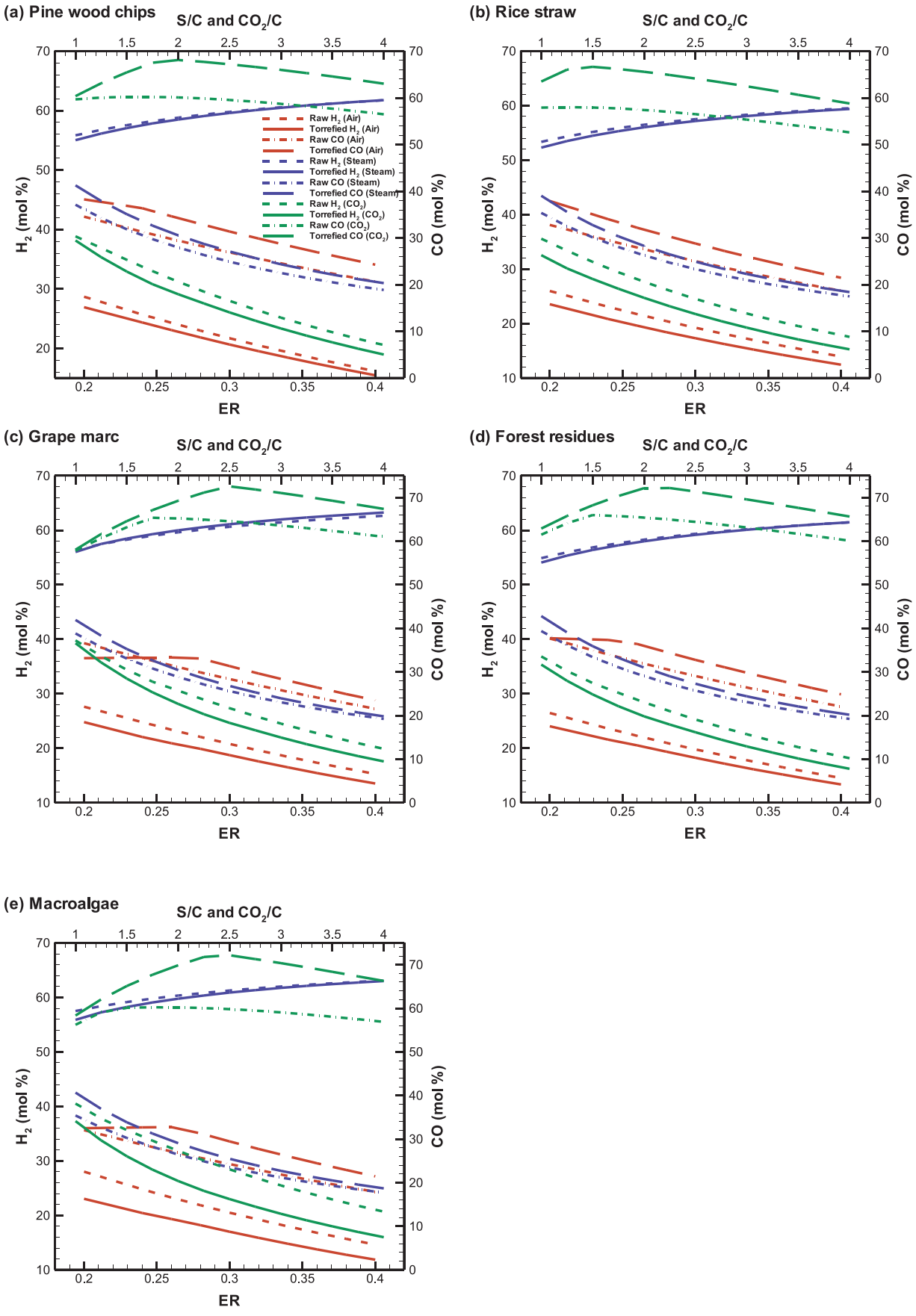

Fig. 1. Effects of the ER, S/C, and CO_2/C ratios on the syngas composition.

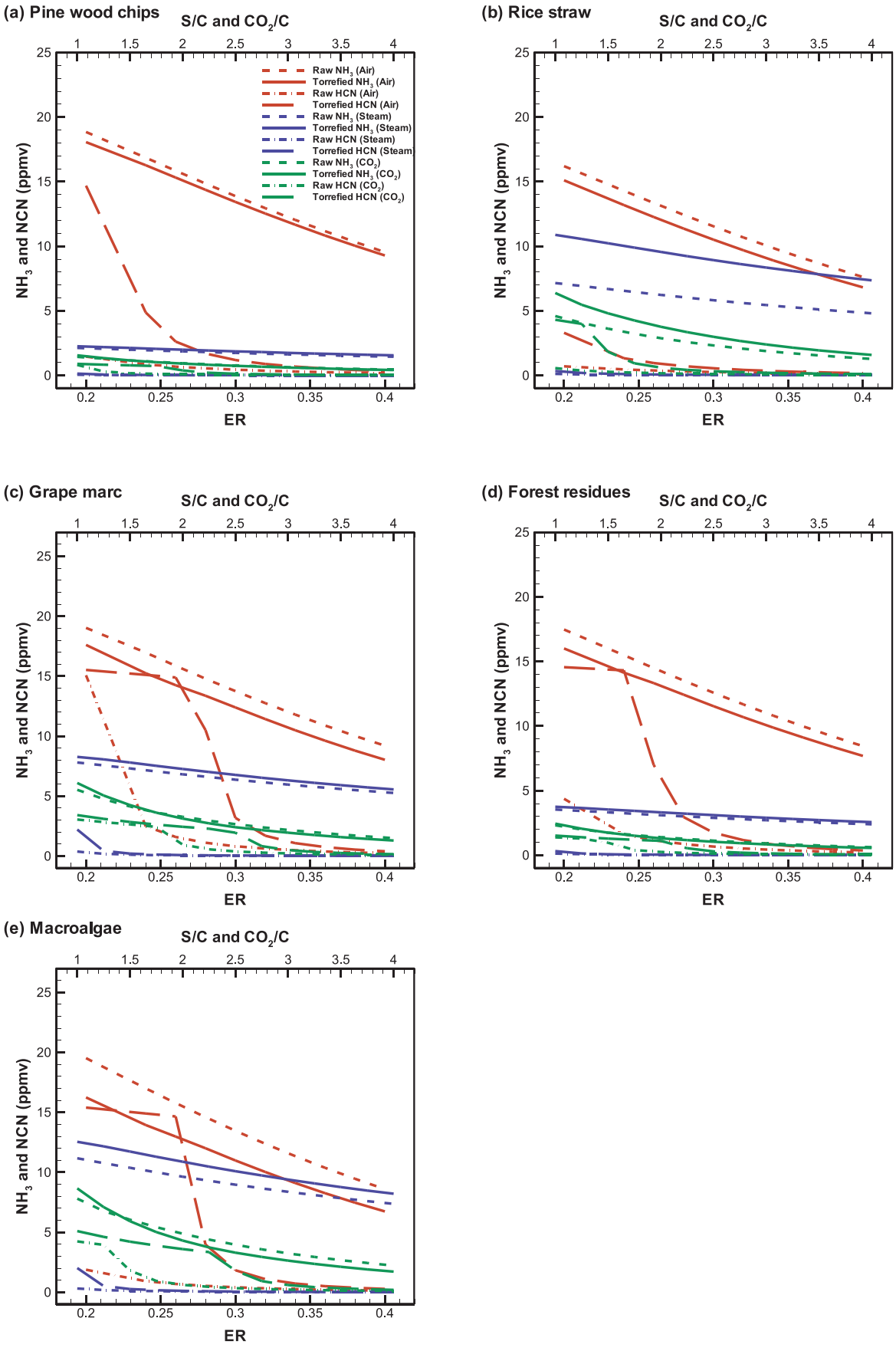

Fig. 2. Effects of the ER, S/C, and CO_2/C ratios on the N-containing compounds.

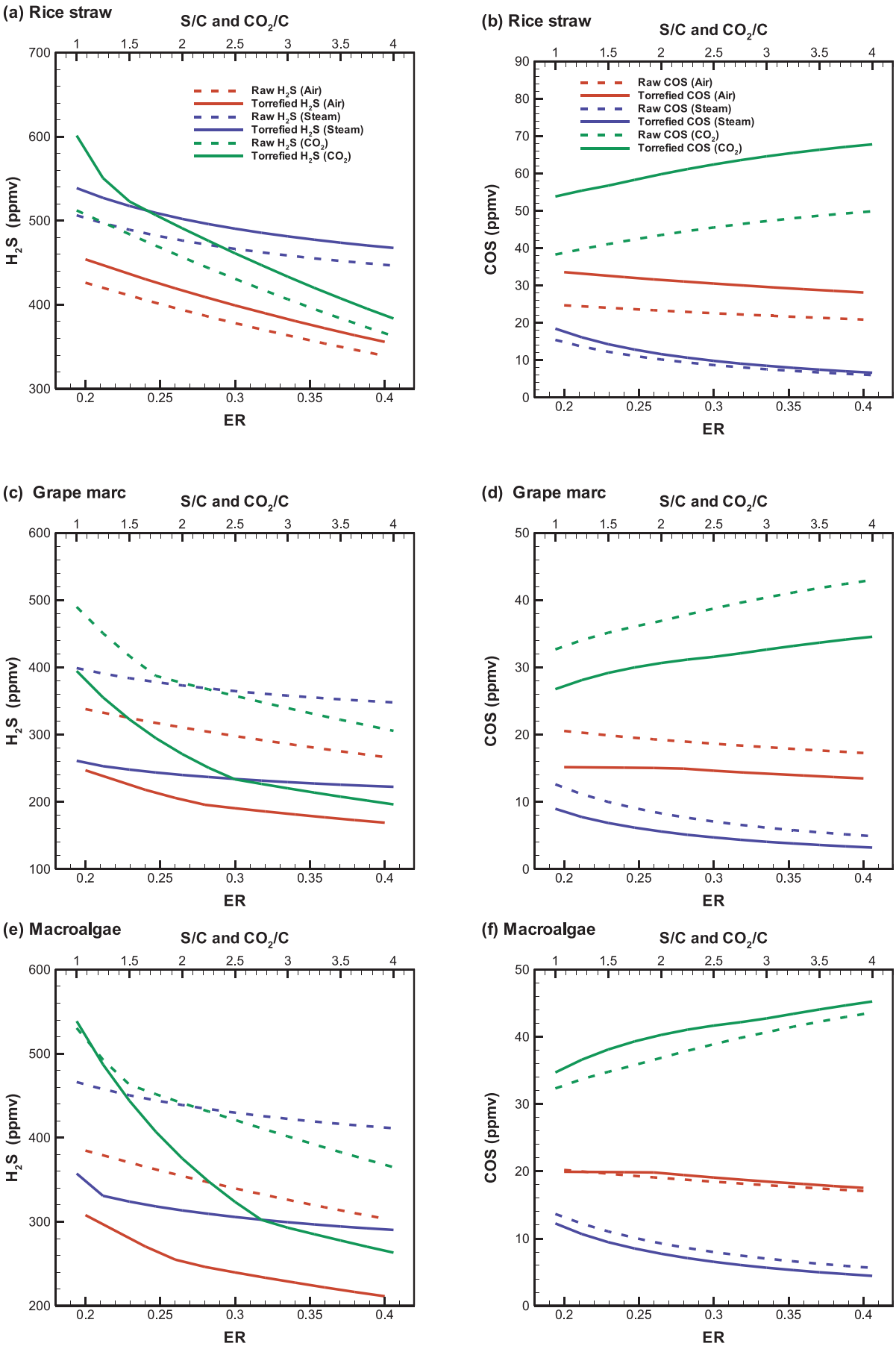

Fig. 3. Effects of the ER, S/C, and CO_2/C ratios on the S-containing compounds.

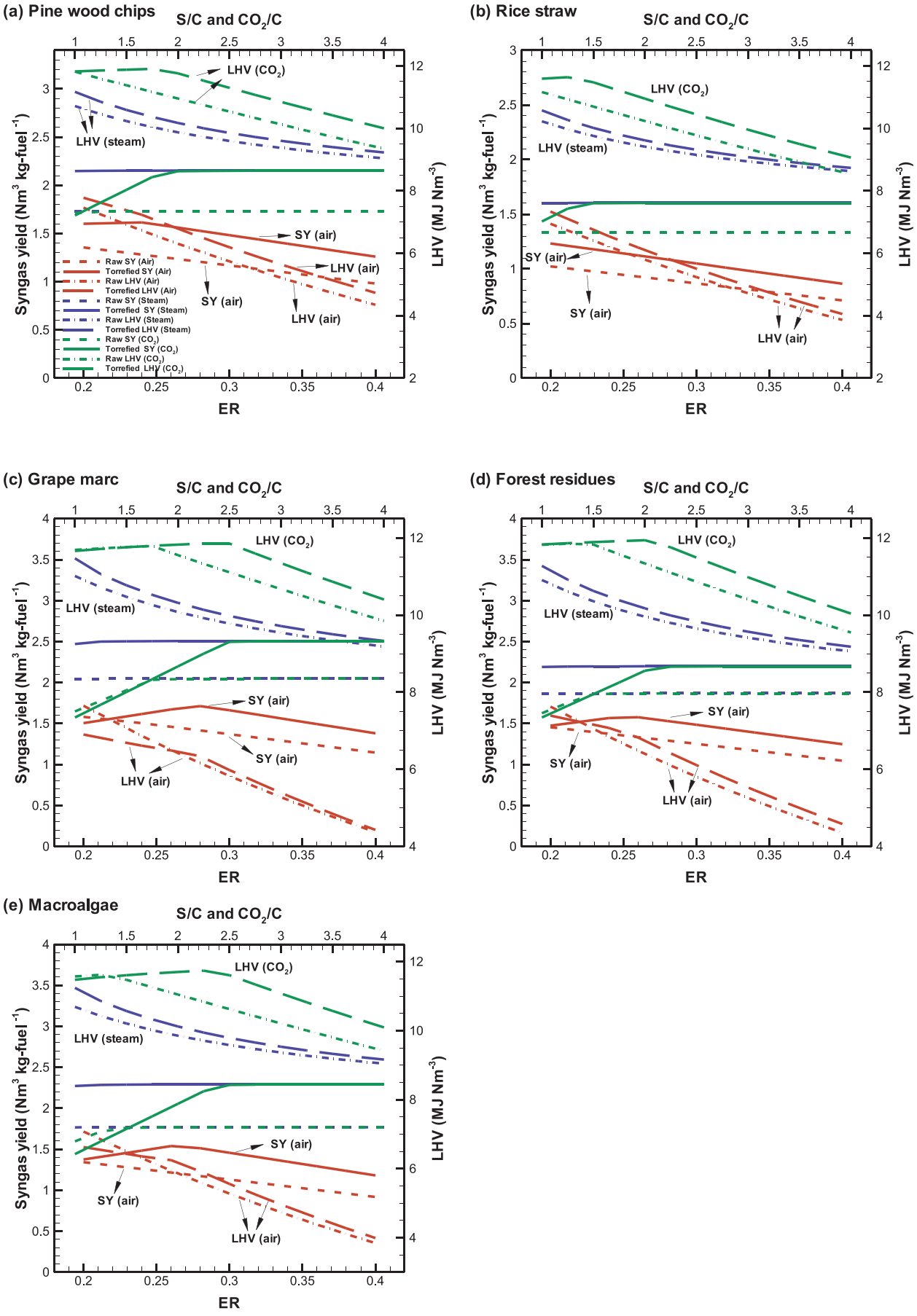

Fig. 4. Effects of the ER, S/C, and CO_2/C ratios on the syngas yield and LHV of the product gas.

Table 4
Comparison of LHV of the product gas of the plasma and conventional gasification at various S/C ratios.

Operating conditions	Plasma gasification LHV (MJ Nm^{-3})									
S/C	RPW	TPW	RRS	TRS	RGM	TGM	RFR	TFR	RMA	TMA
0.5	11.43	11.66	10.91	11.44	11.54	11.48	11.66	11.64	11.44	11.29
1	10.72	11.17	10.23	10.58	11.01	11.47	10.91	11.28	10.69	11.24
1.5	10.23	10.59	9.76	10.01	10.47	10.77	10.36	10.63	10.21	10.57
2	9.87	10.17	9.41	9.61	10.08	10.32	9.96	10.17	9.85	10.12
2.5	9.60	9.86	9.15	9.31	9.78	9.98	9.65	9.83	9.58	9.79
3	9.38	9.60	8.94	9.08	9.54	9.72	9.41	9.57	9.37	9.53
3.5	9.19	9.40	8.77	8.89	9.35	9.50	9.22	9.36	9.19	9.33
4	9.04	9.23	8.63	8.73	9.19	9.33	9.06	9.18	9.04	9.16
Operating conditions	Conventional gasification LHV (MJ Nm^{-3})									
S/C	RPW	TPW	RRS	TRS	RGM	TGM	RFR	TFR	RMA	TMA
0.5	11.05	11.14	10.71	10.60	11.12	11.29	11.04	11.10	11.02	11.06
1	10.79	11.08	10.00	10.65	11.07	11.18	11.00	11.05	10.92	11.02
1.5	9.97	10.54	9.34	9.73	10.39	10.97	10.17	10.62	10.02	10.67
2	9.46	9.87	8.91	9.18	9.76	10.13	9.58	9.88	9.49	9.88
2.5	9.11	9.43	8.62	8.81	9.35	9.62	9.18	9.40	9.14	9.40
3	8.86	9.11	8.40	8.56	9.06	9.27	8.90	9.08	8.88	9.08
3.5	8.67	8.88	8.24	8.36	8.84	9.02	8.70	8.84	8.70	8.84
4	8.52	8.71	8.11	8.22	8.68	8.83	8.53	8.66	8.55	8.67

at lower CO_2/C ratios. Nevertheless, the excess CO_2 fed to the plasma gasifier not only makes R5 more dominant but also dilutes the product gas, causing a significant decrease and increase in CO and CO_2 concentrations, respectively. Similar trends have also been found in the studies of Salaudeen et al. (2018) and Wang et al. (2019). Overall, TGM produces the highest CO concentration of 72.59% at CO_2/C ratio of 2.5, followed by TFR and TMA which are equally 72.17%, at CO_2/C ratios of 2.25 and 2.5, respectively. As mentioned earlier, the maximum values of CO concentration are found at certain CO_2/C ratios where the carbon is completely reacted with CO_2 through R6. Apparently, for the torrefied biomass materials, to achieve a complete carbon-CO_2 reaction, more CO_2 is required to inject into the plasma gasifier. Moreover, the comparative results between raw and torrefied biomass indicate that the H_2 concentration of the former is higher than that of the latter, whereas the CO concentration of the latter is amplified by factors of 0.43–20.64%.

3.1.2. NH_3 and HCN emissions

Fig. 2 plots the distributions of NH_3 and HCN as a function of ER, S/C ratio, and CO_2/C ratio for various raw and torrefied biomass types. The N-containing compounds released from the plasma gasification are highly dependent on the nitrogen content in the feedstock due to the various char-nitrogen reactions (Broer and Brown, 2015). According to the elemental analysis (Table 3), it can be observed that the nitrogen content in the feedstock is increased after torrefaction by about 0.03–3.07 wt%. For the air plasma gasification, it is indicated that NH_3 concentration of all torrefied biomass types is lower than that of raw biomass with the rise of ER, whereas HCN concentration exhibits opposite trends in which its values are increased after torrefaction, especially at lower ERs. The formation of NH_3 and HCN are mainly dominated by R9-R11 during the plasma gasification. These might be due to low hydrogen and high carbon content in the torrefied biomass. It is worthy of note that the extent of decrease in concentration of NH_3 was relatively lower for TPW (by factors of 2.72–4.19%) among the five torrefied biomass samples, while the TMA has the highest reduction in NH_3 emissions (by factors of 16.78–21.69%). Besides, it is apparent that the distributions of HCN formation show two reaction stages, especially for TGM, TFR, and TMA. For example, the concentration of HCN in TGM almost kept constant (i.e. the first stage) in the ER range of 0.2–0.26. This might be attributed to the unconverted char in the plasma gasifier. After completing char conversion, as a result, a sharp decreasing trend of HCN concentration is observed when ER is larger than 0.26 (i.e. the second stage).

Unlike the plasma gasification with air, under steam environment, NH_3 emissions from torrefied biomass are higher than those of raw biomass. Similar results were also found in the study of Pinto et al. (2017b) where the release of NH_3 and H_2S were increased by 54–139% and 91–130%, respectively, during the steam gasification of eucalyptus globulus stumps. The influences of torrefaction on the enhancement factor of NH_3 emissions are ranked as: TRS (52.03–53.36%) > TMA (11.42–13.06%) > TPW (5.94–7.30%)≅TFR (6.18–7.08%) > TGM (5.45–6.69%). However, HCN concentration is barely affected by torrefaction and it is less than 0.3 ppmv when the S/C ratio is larger than 1.5, regardless of what kind of biomass is examined. As regard to the NH_3 emissions under the CO_2 environment, torrefaction has more influence on rice straw and macroalgae. It should be underlined that torrefied biomass has lower NH_3 emissions at higher CO_2/C ratios, except for TMA. For instance, NH_3 emissions from TMA are reduced by factors of 2.03–22.67% when the CO_2/C ratio is operated between 1.5 and 4. As for HCN concentration, torrefied biomass is by far higher than that of a raw one. The enhancement factor of HCN concentration is ranked as: TRS > TMA > TPW > TFR > TGM.

3.1.3. H_2S and COS emissions

The sulfur content in the biomass results in the formation of gaseous sulfides and it is mainly released as H_2S. Non-woody biomass generally contains higher amounts of fuel-S than those of woody biomass (Gai et al., 2014). Similar observations listed in Table 3 shows that only non-woody biomass (RS, GM, and MA) contains significant amounts of sulfur. Fig. 3 shows their distributions of H_2S and COS before and after torrefaction. It is observed that most profiles, with the exception of an opposite trend for COS concentration under CO_2 plasma gasification, decline linearly with process parameters. Furthermore, the effect of three gasifying agents on the sulfur species reveals that for the formation of H_2S during the plasma gasification, using air as a gasifying agent produces the lowest among the three reaction atmospheres, except for RGM and RMA. On the contrary, the formation of COS is the lowest under steam atmosphere, whereas it is the highest under CO_2 atmosphere, as a consequence of the enhanced intensity of R12-R13, thus leading to more COS formation in the product gas

For a comparison of the emissions of H_2S between raw and torrefied materials, the values for the latter are much lower than those of the former. The exception is for TRS, for which torrefaction makes the formation of H_2S and COS increase by factors of 4.87–6.52% and

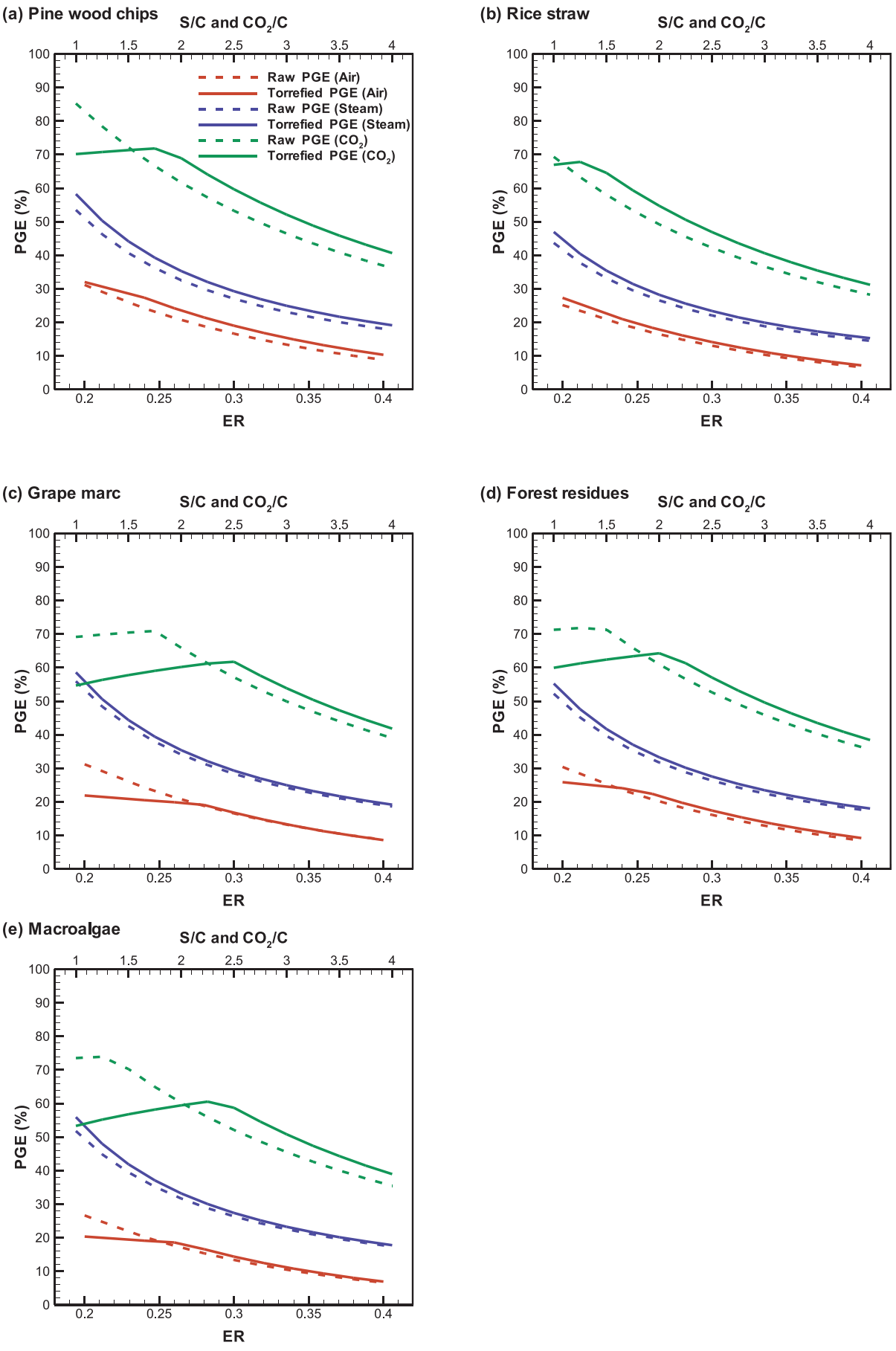

Fig. 5. Effects of the ER, S/C, and CO_2/C ratios on the PGE.

Table 5
Plasma energy to syngas production ratio of raw and torrefied biomass materials.

Operating conditions	Plasma energy to syngas production ratio (kWh kg^{-1})									
	RPW	TPW	RRS	TRS	RGM	TGM	RFR	TFR	RMA	TMA
ER										
0.2	4.43	4.18	4.79	4.32	4.40	5.74	4.25	4.68	5.17	6.07
0.3	7.62	6.61	8.38	7.52	7.53	7.21	7.32	6.66	9.09	8.00
0.4	11.96	10.26	13.47	12.04	11.87	11.41	11.54	10.45	14.71	12.99
S/C										
1	5.18	4.59	6.05	5.47	4.57	4.49	5.09	4.72	4.92	4.59
2	12.35	11.02	14.58	13.37	10.89	10.19	12.28	11.48	11.69	10.08
3	21.25	19.05	25.26	23.34	18.76	17.66	21.29	20.02	20.07	17.48
4	31.69	28.52	37.83	35.15	27.99	26.48	31.90	30.12	29.88	26.22
CO_2/C										
1	1.43	1.67	1.62	1.63	1.67	2.10	1.61	1.86	1.57	2.15
2	2.62	2.33	2.99	2.68	2.33	2.60	2.54	2.41	2.48	2.64
3	3.72	3.33	4.25	3.84	3.31	3.05	3.62	3.37	3.51	3.01
4	4.75	4.28	5.44	4.95	4.24	3.92	4.65	4.34	4.48	3.88

34.81–35.83% in the air atmosphere, 4.69–6.39% and 10.50–19.73% in the steam atmosphere, and 5.78–17.38% and 35.93–40.59% in the CO_2 atmosphere, respectively. These trends were also observed in the study of Pinto et al. (2017a), where H_2S was increased by 100% when torrefied rice husk at 250 °C was gasified. For grape marc, lower amounts of COS are formed after torrefaction, regardless of reaction environment. However, for macroalgae, the amount of COS formation is almost similar for both the RMA and TMA under the air environment, less from TMA in the steam environment, whereas more COS is produced in the CO_2 environment.

3.2. Performance indices of plasma gasification

3.2.1. Syngas yield and LHV of the product gas

Fig. 4 plots the distributions of syngas yield and LHV of the product gas for each biomass along with ER, S/C, and CO_2/C ratios. For air plasma gasification, the values of syngas yield decrease as the ER increases for all types of raw biomass, while those increase and then decrease for torrefied biomass, mainly as a result of an incomplete char reaction. The exception is for TRS which has the lowest carbon content among the five torrefied biomasses. For the steam plasma gasification, the syngas yield is independent of the S/C ratio for all types of biomass. For instance, the syngas yield of RPW and RRS is around 1.73 and 1.33 Nm^3 $kg\text{-}fuel^{-1}$, respectively, no matter what the S/C ratio is. Similar trends are also observed for RPW and RRS under the CO_2 atmosphere (around 1.73 Nm^3 $kg\text{-}fuel^{-1}$ for RPW and 1.33 Nm^3 $kg\text{-}fuel^{-1}$ for RRS), whereas an increasing trend initially at lower CO_2/C ratios and then almost constant for other biomass materials. From the above observations, it is concluded that the syngas yield is marginally promoted by adding excess steam or CO_2 into the plasma gasifier. As a whole, plasma gasification of biomass with air gives the lowest syngas yield, approximately ranging from 0.71 to 1.71 Nm^3 $kg\text{-}fuel^{-1}$, while it is from 1.15 to 2.51 Nm^3 $kg\text{-}fuel^{-1}$ in the steam atmosphere and from 0.96 to 2.50 Nm^3 $kg\text{-}fuel^{-1}$ in the CO_2 atmosphere. Basically, the syngas yield of raw biomass can be enhanced by factors of 7.42–28.90% in the air atmosphere, 17.34–29.47% in the steam atmosphere, and 5.46–29.48% in the CO_2 atmosphere, when biomass is torrefied. Notably, TMA has the highest enhancement factor of syngas yield, regardless of what the gasifying agent is used.

In examining the LHV of the product gas, it decreases linearly along with the ER and S/C ratio for all types of biomass, which is consistent with the observations from the studies of (Favas et al., 2017) and (Ismail et al., 2019). The values of LHV of the product gas ranges from 3.84 to 7.78 MJ Nm^{-3} in the air atmosphere and 8.63–11.47 MJ Nm^{-3} in a steam atmosphere. For the air plasma gasification, the LHV of the product gas for TPM and TRS is higher than that of RPM and RRS, as a result of higher syngas yield, while it happens when the ER is larger than 0.26 for TGM, 0.22 for TFR, and 0.24 for TMA. For the steam plasma gasification, the LHV of the product gas for torrefied biomass is obviously superior to that of raw biomass, no matter which biomass is examined. Moreover, a comparison of the LHV of the product gas between plasma and conventional (700 °C) gasification of various types of biomass is tabulated in Table 4. It is indicated that the values of LHV of the product gas of raw and torrefied biomass from plasma gasification are higher than those from conventional gasification due to the upgraded quality of syngas. These trends are in line with the observations of Janajreh et al., (2013). As regard to the plasma gasification with CO_2, it is found that the distributions of LHV first increase and then decrease substantially. This is due to the fact that the LHV of the product gas is mainly contributed by H_2 and CO, especially the latter (Eq. (4)). Meanwhile, the higher the CO_2/C ratio, the lower the CO concentration in the product gas (Fig. 1). When two factors are concerned together, therefore, the LHV of the product gas goes down after reaching a maximum value. Overall, the LHV of the product gas ranges from 8.54 to 11.94 MJ Nm^{-3} in the CO_2 atmosphere.

3.2.2. PSR and PGE

Fig. 5 shows the plasma gasification efficiency (PGE), and plasma energy to syngas production ratio (PSR) of each biomass material. As expected, the profiles of the PGE are similar to those of LHV of the product gas (Fig. 4). During the plasma gasification, the plasma torch power is also an important input energy source, which will affect the PGE. The values of the PSR of all types of biomass are summarized in Table 5. It can be seen that the values of PSR increase with increasing the process parameters, and those are the lowest under CO_2 atmosphere (1.43–5.44 kWh kg^{-1}), followed by air atmosphere (4.18–14.71 kWh kg^{-1}) and steam atmosphere (4.49–37.83 kWh kg^{-1}). Notably, the values of PSR for some cases are decreased after torrefaction. For example, for TPW, PSR can be reduced by factors of 5.64–14.21%, 10.00–11.39%, and 9.89–11.07%, corresponding to air, steam, and CO_2 atmosphere, respectively. Furthermore, it should be noted that the lowest value of PSR and the highest value of LHV of the product gas are obtained in the CO_2 atmosphere, thereby leading to the highest values in the PGE among the three reaction atmospheres, irrespective of which fuel is used. Although the values of the PSR for steam plasma gasification is the highest, the higher syngas yield causes higher LHV of the product gas, which, in turn, results in the higher PGE as compared to the case of air plasma gasification.

A comparison of PGE between raw and torrefied biomass, for the air plasma gasification, indicates that the values of PGE are increased by factors of 2.79–16.88% for TPW and 8.21–8.59% for TRS. However, TFR and TMA have higher values of PGE when ER is larger than 0.24

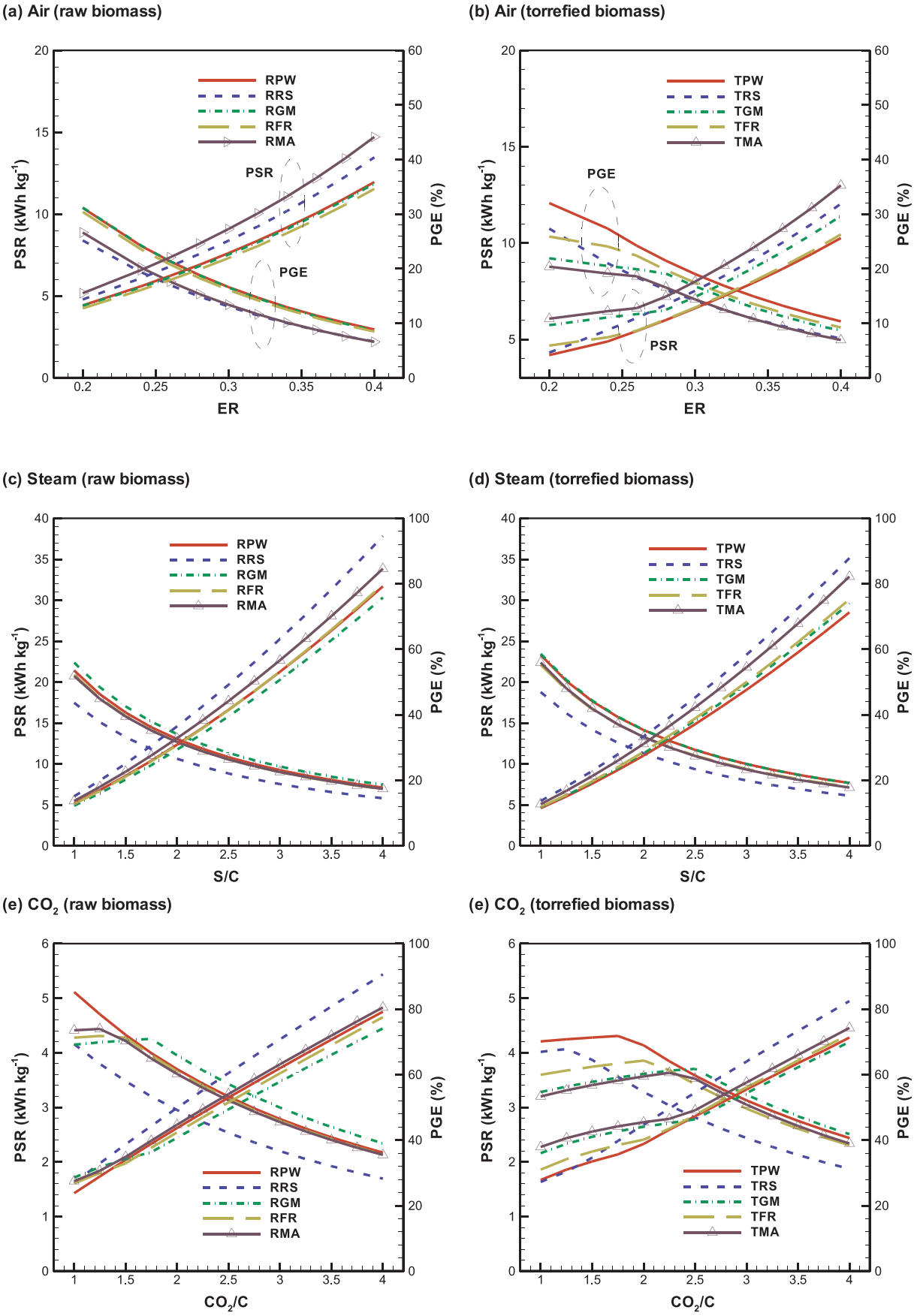

Fig. 6. Comparisons of the PSR and PGE for raw and torrefied biomass under three different gasifying agents.

and 0.26, respectively, whereas the value of PGE for TGM is lower as compared to RGM. For the plasma gasification with steam, using torrefied biomass can improve the PGE by factors of 2.31–8.86%. As far as the plasma gasification with CO_2 is concerned, the PGE is higher than that of raw biomass, when CO_2/C ratio is larger than 1.75 for TPW, 1.25 for TRS, 2.5 for TGM, 2 for TFR, and 2.25 for TMA. It should also be noted that a maximum distribution of PGE is found. This is because an increased syngas yield is observed until it reaches a constant value at certain CO_2/C ratios (Fig. 4), except for RPW and RRS, in which their syngas yield is kept constant throughout the investigated CO_2/C ratio range.

From the above observations, it can be concluded that plasma gasification of raw and torrefied biomass with air is not recommended because of low PGE. In contrast, torrefied biomass is an appropriate fuel for the steam plasma gasification to produce H_2-rich syngas due to its higher syngas yield, LHV of the product gas, and PGE. However, if the PGE, nitrogenous, and sulfur impurities are considered together, TRS is not recommended as a fuel due to higher pollutant emissions. As for the CO_2 plasma gasification, although the maximum value of PGE from torrefied biomass is lower than raw one, TGM and TMA (except for TPW and TFR) are also a promising alternative fuel to replace RGM and RMA as a result of significant reduction in the emissions of total sulfur impurities. It is thus possible to reduce the economic cost of acid gas removal procedures in order to achieve the desired quality of syngas in downstream applications.

3.3. Effect of the biomass type on the plasma gasification performance

In order to find proper feedstocks for the plasma gasification, comparative results in terms of PSR and PGE for five types of raw and torrefied biomass under three different reaction atmospheres are plotted in Fig. 6. For the air plasma gasification, although RFR has the lowest value of PSR, the values of PGE for RPW and RGM are better than RFR. In contrast to raw biomass, TPW has the lowest value of PSR and the highest value of PGE among the five torrefied biomass materials, followed by TFR. For the steam plasma gasification, the values of PGE from the highest to lowest are ranked as RGM > RPW > RFR≅RMA > RRS for raw biomass, while those for torrefied biomass it is TGM≅TPW > TMA≅TFR > TRS. It is noteworthy that the performance of pine wood chips is close to grape marc after torrefaction. With regard to the CO_2 plasma gasification, RPW has the best performance in the CO_2/C ratio range of 1–1.5. Once the CO_2/C ratio is larger than 1.5, RGM is notably superior to other raw biomass materials. Similarly, TPW is better than other torrefied ones when the CO_2/C ratio is controlled between 1 and 2.25, whereas TGM gives the best PGE when the CO_2/C ratio is larger than 2.25. It is thus concluded that pine wood chips have the greatest potential as a fuel for the plasma gasification, whereas rice straw is the least one among the five types of biomass.

In summary, although the combination of biomass torrefaction with plasma gasification is a promising technology to upgrade syngas quality, more investigation with respect to the economic and environmental feasibility of this technology is needed due to an energy-intensive system, and this will be carried out in detail during future research.

4. Conclusions

Different types of raw and torrefied biomass are selected for plasma gasification using three gasifying agents to assess their performances in terms of syngas yield, LHV of the product gas, and PGE. The steam plasma gasification of torrefied biomass is recommended to generate H_2-rich syngas, despite relatively higher amounts of nitrogenous species emitted. Notably, TGM and TMA even have lower sulfur impurities compared to raw state. Moreover, CO_2 plasma gasification suggests the highest value of PGE, whereas using air it is the lowest. From the viewpoints of energy and environment, TPW has the greatest potential for plasma gasification of biomass.

CRediT authorship contribution statement

Po-Chih Kuo: Conceptualization, Writing - review & editing, Funding acquisition. **Biju Illathukandy:** Conceptualization, Writing - review & editing. **Wei Wu:** Conceptualization, Resources, Writing - review & editing. **Jo-Shu Chang:** Conceptualization, Writing - review & editing.

Declaration of Competing Interest

The authors declare that they have no known competing financial interests or personal relationships that could have appeared to influence the work reported in this paper.

Acknowledgments

The authors would like to thank the Ministry of Science and Technology, Taiwan for the financial support of this research under the grant MOST 108-2917-I-564-039.

Appendix A. Supplementary data

Supplementary data to this article can be found online at https://doi.org/10.1016/j.biortech.2020.123740.

References

Broer, K.M., Brown, R.C., 2015. The role of char and tar in determining the gas-phase partitioning of nitrogen during biomass gasification. Appl. Energy 158, 474–483.
Chen, W.H., Kuo, P.C., 2011. Torrefaction and co-torrefaction characterization of hemicellulose, cellulose and lignin as well as torrefaction of some basic constituents in biomass. Energy 36, 803–811.
Diaz, G., Sharma, N., Leal-Quiros, E., Munoz-Hernandez, A., 2015. Enhanced hydrogen production using steam plasma processing of biomass: Experimental apparatus and procedure. Int. J. Hydrogen Energy 40, 2091–2098.
Favas, J., Monteiro, E., Rouboa, A., 2017. Hydrogen production using plasma gasification with steam injection. Int. J. Hydrogen Energy 42, 10997–11005.
Gai, C., Dong, Y., Zhang, T., 2014. Distribution of sulfur species in gaseous and condensed phase during downdraft gasification of corn straw. Energy 64, 248–258.
Guo, P., Saw, W.L., van Eyk, P.J., Stechel, E.B., de Nys, R., Ashman, P.J., et al., 2017. Gasification reactivity and physicochemical properties of the chars from raw and torrefied wood, grape marc, and macroalgae. Energy Fuels 31, 2246–2259.
Hlina, M., Hrabovsky, M., Kopecky, V., Konrad, M., Kavka, T., Skoblja, S., 2006. Plasma gasification of wood and production of gas with low content of tar. In: In: 22nd Symposium on Plasma Physics and. Technology, pp. B1179–B1184.
Hlina, M., Hrabovsky, M., Kavka, T., Konrad, M., 2014. Production of high quality syngas from argon/water plasma gasification of biomass and waste. Waste Manag. 34, 63–66.
Huang, J., Qiao, Y., Wei, X., Zhou, J., Yu, Y., Xu, M., 2019. Effect of torrefaction on steam gasification of starchy food waste. Fuel 253, 1556–1564.
Huang, X., Cheng, D.G., Chen, F., Zhan, X., 2013. Reaction pathways of b-D-glucopyranose pyrolysis to syngas in hydrogen plasma: A density functional theory study. Bioresource Technol. 143, 447–454.
Ismail, T.M., Monteiro, E., Ramos, A., El-Salam, M.A., Rouboa, A., 2019. An Eulerian model for forest residues gasification in a plasma gasifier. Energy 182, 1069–1083.
Janajreh, I., Raza, S.S., Valmundsson, A.S., 2013. Plasma gasification process: Modeling, simulation and comparison with conventional air gasification. Energy Convers. Manage. 65, 801–809.
Kaewluan, S., Pipatmanomai, S., 2011. Potential of synthesis gas production from rubber wood chip gasification in a bubbling fluidised bed gasifier. Energy Convers. Manage. 52, 75–84.
Kai, X., Meng, Y., Yang, T., Li, B., Xing, W., 2019. Effect of torrefaction on rice straw physicochemical characteristics and particulate matter emission behavior during combustion. Bioresource Technol. 278, 1–8.
Kim, K., Kim, Y., Yang, C., Moon, J., Kim, B., Lee, J., et al., 2013. Long-term operation of biomass-to-liquid systems coupled to gasification and Fischer-Tropsch processes for biofuel production. Bioresource Technol. 127, 391–399.
Kuo, P.C., Wu, W., Chen, W.H., 2014. Gasification performances of raw and torrefied biomass in a downdraft fixed bed gasifier using thermodynamic analysis. Fuel 117, 1231–1241.
Li, T., Wang, L., Ku, X., Guell, B.M., Løvås, T., Shaddix, C.R., 2015. Experimental and modeling study of the effect of torrefaction on the rapid devolatilization of biomass. Energy Fuels 29, 4328–4338.
Liu, M., Aravind, P.V., 2014. The fate of tars under solid oxide fuel cell conditions: A

review. Appl. Therm. Eng. 70, 687–693.
Marcello, M.D., Tsalidis, G.A., Spinelli, G., de Jong, W., Kiel, J.H.A., 2017. Pilot scale steam-oxygen CFB gasification of commercial torrefied wood pellets. The effect of torrefaction on the gasification performance. Biomass Bioenergy 105, 411–420.
Mazzoni, L., Janajreh, I., 2017. Plasma gasification of municipal solid waste with variable content of plastic solid waste for enhanced energy recovery. Int. J. Hydrogen Energy 42, 19446–19457.
Minutillo, M., Perna, A., Bona, D.D., 2009. Modelling and performance analysis of an integrated plasma gasification combined cycle (IPGCC) power plant. Energy Convers. Manage. 50, 2837–2842.
Misljenovic, N., Bach, Q.V., Tran, K.Q., Salas-Bringas, C., Skreiberg, O., 2014. Torrefaction influence on pelletability and pellet quality of norwegian forest residues. Energy Fuels 28, 2554–2561.
Munir, M.T., Mardon, I., Al-Zuhair, S., Shawabkeh, A., Saqib, N.U., 2019. Plasma gasification of municipal solid waste for waste-to-value processing. Renew. Sustain. Energy Rev. 116 109461.
Oh, S.Y., Yun, S., Kim, J.K., 2018. Process integration and design for maximizing energy efficiency of a coalfired power plant integrated with amine-based CO_2 capture process. Appl. Energy 216, 311–322.
Park, D.C., Day, S.J., Nelson, P.F., 2008. Formation of N-containing gas-phase species from char gasification in steam. Fuel 87, 807–814.
Phanphanich, M., Mani, S., 2011. Impact of torrefaction on the grindability and fuel characteristics of forest biomass. Bioresource Technol. 102, 1246–1253.
Pinto, F., Gominho, J., Andre, R.N., Gonçalves, D., Miranda, M., Varela, F., et al., 2017a. Effect of rice husk torrefaction on syngas production and quality. Energy Fuels 31, 5183–5192.
Pinto, F., Gominho, J., Andre, R.N., Gonçalves, D., Miranda, M., Varela, F., et al., 2017b. Improvement of gasification performance of Eucalyptus globulus stumps with torrefaction and densification pre-treatments. Fuel 206, 289–299.
Ren, X., Sun, R., Meng, X., Vorobiev, N., Schiemann, M., Levendis, Y.A., 2017. Carbon, sulfur and nitrogen oxide emissions from combustion of pulverized raw and torrefied biomass. Fuel 310–323.
Rios, M.L.V., González, A.M., Lora, E.E.S., Olmo, O.A.A.D., 2018. Reduction of tar generated during biomass gasification: A review. Biomass Bioenergy 108, 345–370.
Salaudeen, S.A., Acharya, B., Heidari, M., Arku, P., Dutta, A., 2018. Numerical investigation of CO_2 valorization via the steam gasification of biomass for producing syngas with flexible H_2 to CO ratio. J. CO_2 Util. 27, 32–41.
Shie, J.L., Tsou, F.J., Lin, K.L., Chang, C.Y., 2010. Bioenergy and products from thermal pyrolysis of rice straw using plasma torch. Bioresource Technol. 101, 761–768.
Wang, M., Mao, M., Zhang, M., Wen, G., Yang, Q., Su, B., et al., 2019. Highly efficient treatment of textile dyeing sludge by CO_2 thermal plasma gasification. Waste Manage. 90, 29–36.
Weiland, F., Nordwaeger, M., Olofsson, I., Wiinikka, H., Nordin, A., 2014. Entrained flow gasification of torrefied wood residues. Fuel Process. Technol. 125, 51–58.
Xi, D., Zhou, R., Zhou, R., Zhang, X., Ye, L., Li, J., et al., 2017. Mechanism and optimization for plasma electrolytic liquefaction of sawdust. Bioresource Technol. 241, 545–551.
Xue, G., Kwapinska, M., Horvat, A., Kwapinski, W., Rabou, L.P.L.M., Dooley, S., et al., 2014. Gasification of torrefied Miscanthusgiganteus in an air-blown bubbling fluidized bed gasifier. Bioresource Technol. 159, 397–403.